

## Determination of the relaxation characteristics for solvents from non-stationary spectra: the role of the gating pulse duration

© I.P. Yermolenko, V.A. Mikhailova,<sup>✉</sup> A.I. Ivanov

Volgograd State University,  
400062 Volgograd, Russia

<sup>✉</sup> e-mail: mikhailova.va@volsu.ru

Received July 15, 2022

Revised July 15, 2022

Accepted August 25, 2022

The previously developed approach to the analysis of experimental spectra of non-stationary fluorescence has been improved by taking into account the effect of the duration of the gating pulse and a more accurate description of the initial stage of solvent relaxation. The exponential function used to describe the inertial component of relaxation has been replaced by the Gaussian function. This approach explicitly takes into account the reorganization and relaxation of the solvent and intramolecular vibrations. It includes an explicit description of the wave packet formation in the excited state of the fluorophore. The improvement of the approach made it possible to refine the relaxation characteristics of a number of solvents: ethylene glycol, dimethyl sulfoxide, butyronitrile, ethyl acetate, diethyl ether, dipropyl ether.

**Keywords:** nonequilibrium of the nuclear subsystem, Stokes shift, relaxation of intramolecular vibrations, inertial component of solvent relaxation

DOI: 10.21883/EOS.2022.10.54860.3924-22

### Introduction

The rapid development of laser technology with a femtosecond time resolution has expanded the possibilities for recording and studying in detail the dynamics of ultrafast chemical transformations, which, as a rule, occur under nonequilibrium conditions. „Hot “ spectroscopy methods developed back in the 1960s [1, 2] made it possible to measure, for example, the relaxation characteristics of a solvent. The interest of experimenters and theorists in the study of photoinduced ultrafast reactions associated, in particular, with the transfer of an elementary charge (electron and/or proton), currently continues to increase, since this class of processes is widespread in living and inanimate nature [3–14]. It is well known that the dynamics of ultrafast electron transfer in donor-acceptor systems in condensed media strongly depends on the dynamic properties of the environment [2,5,7–12]. Since the transferred electron interacts with a large number of nuclear degrees of freedom of the donor, acceptor, and surrounding molecules of the medium, the reaction dynamics is determined by numerous parameters determined by the dynamic properties of the solvent and the characteristics of intramolecular vibrations. To quantitatively calculate the dynamics of ultrafast electron transfer reactions, it is necessary to know all these parameters. In polar media, where the long-range Coulomb interaction of the transferred charge with the polarization of the medium predominates, the necessary information about the dynamic properties of the medium is contained in one quantity i.e. in the complex permittivity of the medium  $\varepsilon(\omega)$  [15]. It expresses the electron transfer rate constant, the dissipative properties of

the medium (generalized electron friction coefficients and reaction coordinates) [16] and the spectral dynamics of fluorescence [17–23]. However, due to spatial dispersion, the use of macroscopic permittivity leads to significant errors. The necessary information about the microscopic relaxation characteristics of the medium is contained in the spectral dynamics of fluorescence.

Theoretical approaches to the description of spectral dynamics are currently well developed [17–20] and are successfully used to model it in real systems [21–25]. Information on the relaxation of the solvent and the photo-excited molecule is contained in the spectral dynamics of fluorescence [26]. The dynamics for the shift of the maximum of the fluorophore's fluorescence spectrum, as a rule, is identified with the dynamics of the relaxation of the medium, although recent studies show a significant contribution of intramolecular relaxation [26,27]. Experiments and computer simulations of molecular dynamics indicate that this shift is well approximated by the function [26–28]

$$Q(t) = x_1 \exp(-(t/\tau_1)^2) + \sum_{i=2}^N x_i \exp(-t/\tau_i), \quad (1)$$

including the Gaussian function to describe the fastest relaxation component ( $\tau_1 < \tau_i, i > 1$ ). This component corresponds to the inertial motion of solvent molecules [26,27].

Recently in ref [24], within the framework of perturbation theory based on the operator of a molecule interaction with an exciting pulse, an approach for modeling the spectrum of non-stationary fluorescence, was developed. This approach includes the description of both the solvent relaxation and the relaxation of intramolecular vibrations. Since

intramolecular relaxation makes a significant contribution to the spectral dynamics of fluorescence at short times, this approach makes it possible to significantly improve the accuracy of determining the relaxation times of fast solvent modes [25].

In the works [24,25] the inertial relaxation of the solvent was simulated by exponential function. This could be one of the reasons for the problems in describing the spectral dynamics of perylenedimethylaniline fluorescence for short periods of time [25]. The purpose of this work is to study: (1) manifestations of the inertial motion of solvent molecules in the spectra of non-stationary fluorescence, (2) the scale of changes in the solvent relaxation time after replacing the exponential function describing the fastest relaxation component with the Gaussian function using the analysis of experimental fluorescence spectra of coumarin 153 (C153) as an example, (3) the influence of the duration of the gating pulse, which provides the time window, for the solvent relaxation time. This will improve the methodology for determining the true values of the relaxation parameters of the solvent from the experimental spectra.

## Model and theoretical aspects of the dynamics for non-stationary fluorescence spectra

This section presents a brief description of the model developed in [24]. Model includes: 1) two electronic states ( $|1\rangle$  is excited and  $|2\rangle$  is ground), 2) interaction of the electronic sub-system with the medium is considered as linear, 3) the influence of the medium and all active intramolecular vibrational modes is simulated through interaction with a set of harmonic oscillators with a specially selected spectral density. The spectral density determines the dynamic properties of the medium and allows one to relate them to the spectral dynamics. The reorganization of intramolecular vibrations and their relaxation also affect the spectral dynamics of fluorescence. Therefore, the separation of their contributions in the experimental spectra is still an unsolved problem.

In the diabatic basis, the Hamiltonian of the considered electronic oscillatory system has the form [29–34]

$$H = V_{12}\sigma_+ + V_{21}\sigma_- + \frac{(\sigma_z - 1)}{2} \times \left( \Delta E + \sum_j A_j x_j \right) + H_1, \quad \Delta E = E_1 - E_2 - E_r, \quad (2)$$

where  $E_r = \sum_j A_j^2 / 2\omega_j^2$  is the reorganization energy of all nuclear degrees of freedom,  $H_1 = \sum (p_j^2/2 + x_j^2\omega_j^2/2)$  is Hamiltonian of the vibrational subsystem for excited electronic state  $|1\rangle$ . The Pauli matrices  $\sigma_z$ ,  $\sigma_\pm$  play the role of dynamic variables of the electronic subsystem, the intrinsic states of the matrix correspond to the considered states of the electronic subsystem ( $|1\rangle$  and  $|2\rangle$ ) with eigenvalues

$E_1$  and  $E_2$ . Further, only the  $\Delta E$  parameter is specified. Accordingly, the Hamiltonian of the vibrational subsystem for the electronic state  $|2\rangle$  can be presented in the form

$$H_2 = H_1 - \sum_j A_j x_j - \Delta E.$$

$V_{12} = \langle 1|V(t)|2\rangle$  and  $V_{21}$  are electronic matrix inter-state transition elements. In the Condon approximation, one choose the operator  $V(t)$  in the form  $V = \mathbf{dE} = V_0 \exp(i\omega_e t - t^2/\tau_e^2)$ ,  $\mathbf{d}$  is the dipole moment of the molecule,  $\mathbf{E}$  is the electric field strength of the excitation pulse with the carrier frequency  $\omega_e$  and duration  $\tau_e$ ,  $V_0$  is the maximum value of the interaction between the electric field of the pumping pulse and the dipole moment of the dissolved molecule. Parameters  $x_j$ ,  $p_j$ ,  $\omega_j$ ,  $A_j$  are generalized coordinates, momenta, frequencies of oscillators simulating the influence of the medium and other nuclear degrees of freedom of the system (low- and high-frequency oscillations), and the parameters of the electronic-vibrational bond.

Note that to describe the evolution of the electronically excited state of a molecule, there is no need to determine the entire set of parameters characterizing the nuclear subsystem and its interaction with the electronic sub-system. All the necessary information is contained in the spectral density of oscillators [30]

$$J(\omega) = \frac{1}{2} \sum_j \frac{A_j^2}{\omega_j} \delta(\omega - \omega_j). \quad (3)$$

Further, using linear transformations of the form  $y_1 = \sum A_j x_j / \lambda$ ,  $\lambda^2 = \sum A_j^2$ , one can pass to a model in which only one collective degree of freedom, described by the reaction coordinate  $y_1$ , interacts with the electron subsystem [35,36]. The introduced collective degree of freedom  $y_1$  can exchange energy and momentum with other nuclear degrees of freedom. The fluorescence spectrum is completely determined by the distribution of particles along this coordinate.

Within the model (2) the dynamics of non-stationary fluorescence spectra of molecular compounds in liquid media can be described using an analytical expression obtained earlier in the framework of perturbation theory [24]:

$$I_0 \sim \omega^3 \sum_{n,m} F(\mathbf{n}, \mathbf{m}) \Phi(\omega, t, \mathbf{n}, \mathbf{m}). \quad (4)$$

Here  $F(\mathbf{n}, \mathbf{m})$  — is the Franck-Condon factor [37], which takes into account the difference in the frequencies of intramolecular vibrations  $\Omega_\beta^i$  in excited ( $i = 1$ ) and ground ( $i = 2$ ) states  $\Omega_\beta^{(1)} \neq \Omega_\beta^{(2)}$  [38]. Vector arguments  $\mathbf{n} = (n_1, \dots, n_b, \dots, n_M)$ ,  $\mathbf{m} = (m_1, \dots, m_\beta, \dots, m_M)$  denote the set of vibrational sublevels,  $M$  is the number of active high-frequency intramolecular vibrations in the  $i$ -th electronic state. It should be emphasized that only high-frequency oscillations ( $\hbar\Omega_\beta^{(1)} \gg k_B T$ ) are taken into account

below. Here  $\hbar$  is Planck's constant,  $T$  is temperature,  $k_B$  is Boltzmann's constant. The manifestation of low-frequency oscillations in non-stationary fluorescence spectra within the framework of this theory was studied in the work [39]. The function  $\Phi$  in formula (4)

$$\Phi(\omega, t, \mathbf{n}, \mathbf{m}) = \int_{-\infty}^t d\xi P \left( \hbar\omega + E_r + \Delta G + \sum_{\beta} n_{\beta} \hbar\Omega_{\beta}^{(2)} - \sum_{\beta} m_{\beta} \hbar\Omega_{\beta}^{(1)}, t, \xi, \mathbf{m} \right) \quad (5)$$

is expressed in terms of the function  $P$ , to determine which the equation describing the relaxation of high-frequency vibrational modes is solved,

$$\begin{aligned} \frac{dP(y_1, t, \xi, \mathbf{m})}{d\xi} = & \sum_{\beta=1}^M \left[ \frac{m_{\beta} + 1}{\tau_{v\beta}} P(y_1, t, \xi, \mathbf{m}'_{\beta}) + \frac{m_{\beta} - 1}{\tau_{v\beta}^u} P(y_1, t, \xi, \mathbf{m}''_{\beta}) - m_{\beta} \left( \frac{1}{\tau_{v\beta}^u} + \frac{1}{\tau_{v\beta}^d} \right) \right. \\ & \left. \times P(y_1, t, \xi, \mathbf{m}) \right] + Z_e^{-1} \varphi_0(y_1, t, \xi, \mathbf{m}). \end{aligned} \quad (6)$$

Here the vector  $\mathbf{m}$  differs from  $\mathbf{m}'_{\beta} = (m_1, \dots, m_{\beta} + 1, \dots, m_M)$  and  $\mathbf{m}''_{\beta} = (m_1, \dots, m_{\beta} - 1, \dots, m_M)$  only by an additional quantum in  $\beta$ -th vibrational mode, the rate constants of the downward and upward vibrational transitions are  $m_{\beta}/\tau_{v\beta}^d$  and  $m_{\beta}/\tau_{v\beta}^u$  respectively (in Fig. 1 these transitions are schematically shown by arrows with indices:  $d$  — with the annihilation of a vibrational quantum,  $u$  — with the birth of a vibrational quantum). Under conditions of thermodynamic equilibrium,  $\tau_{v\beta}^u$  and  $\tau_{v\beta}^d$  are related by the relation  $\tau_{v\beta}^u/\tau_{v\beta}^d = \exp(\hbar\Omega_{\beta}^{(1)}/k_B T)$ . Next, an approximation is used (Fig. 1), which makes it possible to ignore transitions with thermal production of a high-frequency quantum (arrow with index  $u$  in Fig. 1).

The function  $\varphi_0(y_1, t, \xi, \mathbf{m})$  in equation (6) describes the distribution of „particles“ along the reaction coordinate  $y_1$  in the vibrational state  $\mathbf{m}$  of the excited electronic state:

$$\begin{aligned} \varphi_0(y_1, t, \xi, \mathbf{m}) = & \frac{F(0, \mathbf{m})}{\sigma_e(t - \xi)} \\ & \times \exp \left\{ -\frac{y_1 - eE_{rm}Q(t - \xi)^2}{2E_{rm}k_B T} - \frac{2\xi^2}{\tau_e^2} - \frac{\hbar^2 \delta\omega_e^2(t - \xi, \mathbf{n})}{2\sigma_e^2(t - \xi)} \right\}, \end{aligned} \quad (7)$$

where  $\hbar\delta\omega_e(t) = \hbar\omega_e + \Delta G - E_{rm} - y_1 Q(t)$ ,  $y_1 = \hbar\omega + E_{rm} + \Delta G + \sum_{\beta} n_{\beta} \hbar\Omega_{\beta}^{(2)} - \sum_{\beta} m_{\beta} \hbar\Omega_{\beta}^{(1)}$ ,  $\sigma_e^2(t) = 2E_{rm}k_B T(1 - Q^2(t)) + \hbar^2 \tau_e^{-2}$ ,  $Z_e^{-1}$  is normalization factor, and the function  $Q(t)$ , which describes the relaxation of the solvent,

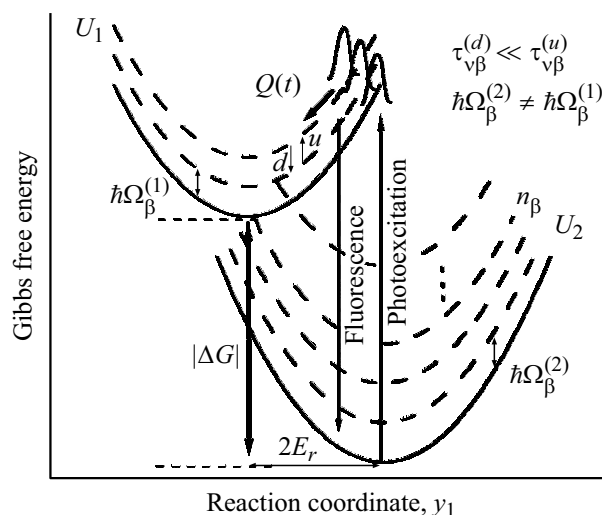


**Figure 1.** Gibbs free energy profiles along the reaction coordinate  $y_1$  for excited  $U_1$  and ground  $U_2$  electronic states. The dashed curves show the vibrationally excited states with the frequency  $\Omega_{\beta}^{(i)}$  for the considered electronic states ( $\Omega_{\beta}^{(1)} \neq \Omega_{\beta}^{(2)}$ ). Schematically (vertical arrows) shows the vibrational relaxation of high-frequency modes (arrows with indices:  $u$  — with the destruction of a vibrational quantum,  $d$  — with the birth of a vibrational quantum), as well as photo-excitation and fluorescence.

is determined in terms of the spectral density of oscillators

$$Q(t) = \frac{1}{\pi E_{rm}} \int_0^{\infty} \frac{J(\omega)}{\omega} \cos \omega t d\omega. \quad (8)$$

Here  $E_{rm}$  is the solvent reorganization energy. In the case of multi-exponential relaxation,

$$Q(t) = \sum_{i=1}^N x_i \exp(-t/\tau_i), \quad (9)$$

where  $x_i$  and  $\tau_i$  are the weights and relaxation times of the solvent collective modes, the spectral density has the form

$$J_D(\omega) = 2E_{rm} \sum_{i=1}^N x_i \frac{\omega^2 \tau_i}{1 + \omega^2 \tau_i^2}. \quad (10)$$

In actual systems, the exponential stage of shifting the spectrum maximum is reached only at significant times [26,40,41]. To describe the fastest relaxation component ( $\tau_1 < \tau_i$ ,  $i > 1$ ) associated with the inertial motion of solvent molecules, the Gauss function (1) should be used, so the function  $J(\omega)$  should look like this [26,27]

$$\begin{aligned} J_G(\omega) = & E_{rm} x_1 \sqrt{\pi} \omega^2 \tau_1 \exp(-\omega^2 \tau_1^2 / 4) \\ & + E_{rm} \sum_{i=2}^N x_i \frac{2\omega^2 \tau_i}{1 + \omega^2 \tau_i^2}. \end{aligned} \quad (11)$$

The difference in the character of inertial and diffusion (9) motions is reflected, for example, in the probabilities of „hot“ nonradiative electronic transitions [41].

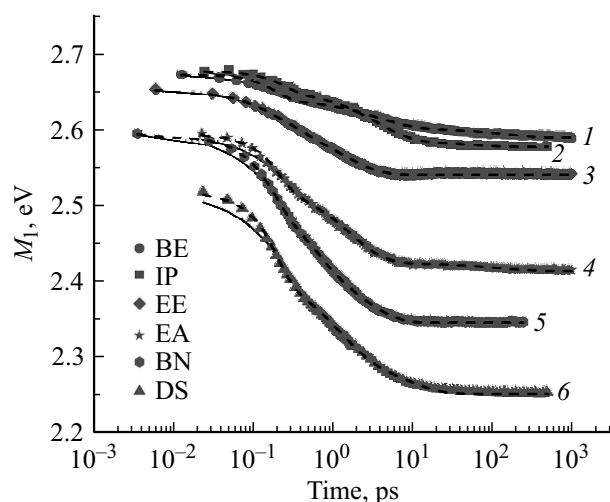


**Figure 2.** Time dependences of the first moments  $M_1(t)$  of the spectra of the C153 molecule in various solvents: 1 is dibutyl ether (BE), 2 is dipropyl ether (IP), 3 is ethyl ether (EE), 4 is ethyl acetate (EA), 5 is butyronitrile (BN), 6 is dimethyl sulfoxide (DS). Experimental data [24] are shown by symbols, approximation are by solid ones (model (9)) and by dashed ones (model (1)) curves.

In this work, based on the fitting of the experimental spectral dynamics of the C153 molecule by the multi-dimensional optimization method performed within the framework of the model with the Gaussian form for the inertial component of the solvent relaxation (1) and taking into account the finite duration of the gating pulse, the parameters of the relaxation function  $Q(t)$  are refined: relaxation times  $\tau_i$  and weights  $x_i$  of each component for a number of solvents. In addition, the scale of the error in determining the parameters of the medium relaxation function introduced by replacing the Gaussian function with exponential function to describe the inertial relaxation component is determined.

The code that implements this approach is described in detail in [42]. It should be emphasized that during these calculations, the solvent reorganization energy  $E_{rm}$ , the exergonicity parameter  $-\Delta G$ , and the characteristics of high-frequency intramolecular modes (frequencies, their weights, total reorganization energy  $E_{rv}$ ) did not varied. They were determined earlier from experimental stationary absorption and fluorescence spectra [24].

## Results and discussion

The main results of fitting the model spectra (4)–(8) to the experimental data are presented in Fig. 2–4, as well as in the additional material (the link to the file can be found in the online version). The experimental spectra were published in the work [24]. As a rule, in order to extract information about the relaxation dynamics of a solvent, the spectra are not analyzed completely i.e. only the dynamics

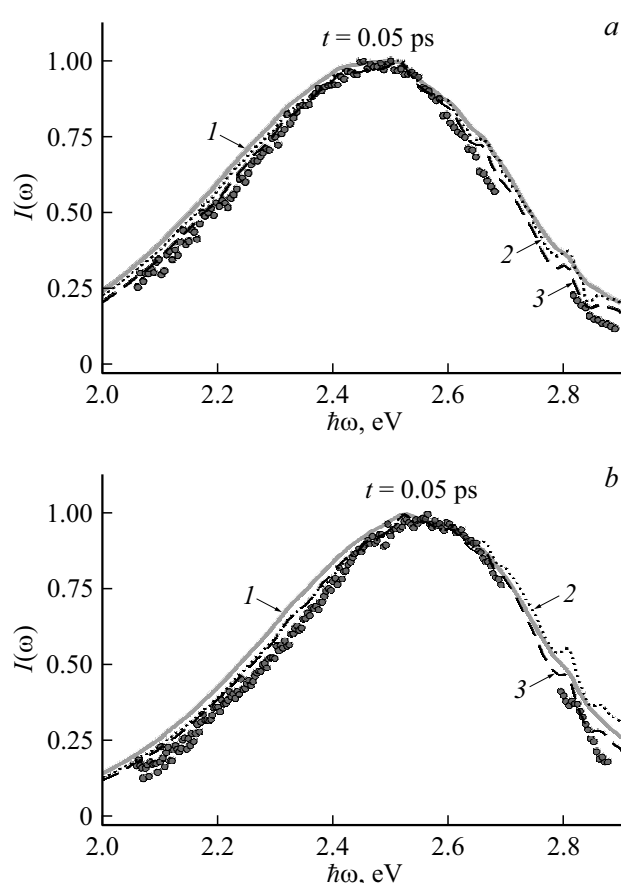


**Figure 3.** Profile of the fluorescence spectrum in DS (panel a), in BN (panel b) after a time interval of 0.05 ps after photo-excitation. Experimental data [24] are shown with symbols. Solid gray curve 1 is approximation using the model (9), dotted curve 2 is approximation using the model (1), dashed curve 3 is the model (1) using convolution (10).

of their spectral moments and/or maxima is studied [26]. It is believed that the dynamics of the first moment of the  $M_1(t)$  fluorescence spectrum is practically independent of the presence or absence of vibrational relaxation [8], which can introduce significant errors into the obtained values of the relaxation characteristics of the solvent. At the same time, the shape of the non-stationary spectrum (the evolution of its width and asymmetry) depends on the state of intramolecular vibrations, therefore, modeling the entire spectral dynamics of fluorescence allows one to obtain information not only about vibrational relaxation, but also refines the relaxation characteristics of the solvent [24].

For a preliminary assessment of the possibility of simulating the initial stage of medium relaxation within the framework of models (1) and (9), an approximation was made of the time dependence of the first moment of the experimental fluorescence spectra  $M_1(t)$  (Fig. 2) in solvents different degrees of polarity. Numerical calculations show that the medium relaxation models (9) (solid lines) and (1) (dashed lines) at early times predict qualitatively different behavior of the first momentum  $M_1(t)$ . The Gaussian

function gives a quadratic time dependence  $\ln M_1(t)$ , while the exponential function gives a linear one. The experimental data unambiguously confirm the quadratic dependence (Fig. 2 and S2, see file ESM1.pdf). Thus, the choice of a function to describe the solvent relaxation at the initial stage of evolution can qualitatively change the behavior of the spectral dynamics.

The results of fitting expressions (4)–(8) to the experimental dynamics for the spectra of coumarin 153 in DS and BN solvents are shown in Fig. 3, 4. This makes it possible „to see“ the manifestation of the inertial motion of solvent molecules in the fluorescence spectra of coumarin at short delay times ( $t \ll 1$  ps). At the initial stage of the evolution of the fluorescence spectra, a vibrational structure appeared (dashed curves 2 in Fig. 3). In the experimental spectra (symbols), this structure is not visible. This difference can be explained by the comparability of the relaxation time of intramolecular vibrations with the duration of the pumping pulse ( $\tau_e = 0.1$  ps) and the gating pulse. In order to take into account the finiteness of the time, the spectrum

profile (4) was convolved with the gating pulse profile:

$$I(\omega, t) = \int_{-\infty}^{\infty} I_0(\omega, t - \eta) \exp\left(-\frac{\eta^2}{2\tau_f}\right) d\eta \quad (12)$$

( $\tau_f = 0.1$  ps is the duration of the gating pulse used in the experiment, which provides the time window), which led to a smoothing of the spectrum shape (dashed curve 3 in Fig. 3). The evolution of fluorescence spectra during large times is well simulated within both models (1) and (9) (see file ESM 1.pdf).

The matching of the calculated non-stationary fluorescence spectra (4)–(8) to the experimental ones performed according to the new algorithm made it possible to significantly improve the quality of the fitting. The approximation error of the spectra observed after a time interval of 0.05 ps after photo-excitation decreased on average by a factor of 2. This made it possible to refine the relaxation parameters of a number of solvents (ethylene glycol, dimethyl sulfoxide, butyronitrile, ethyl acetate, ethyl ether, dipropyl ether) of various degrees of polarity (Table).

As follows from the results (table), the parameters  $x_i$ ,  $\tau_i$  of all investigated solvents, except for ethyl ether (EE) and ethylene glycol (EG), changed significantly. For example, the relaxation time of the first component of dimethyl sulfoxide (DS) increased by 19%, and its weight decreased by 20%, but the other components also changed. For butyronitrile (BS), the parameter  $\tau_1$  increased by 12%, and the weight of  $x_1$  decreased by 30%. All these changes are associated with a more accurate description of the initial stage of solvent relaxation and allowance for the effect of the length of the gating pulse.

It should be noted that approximations of the first moment  $M_1(t)$  and the spectrum profile in the solvent EE using both relaxation models (1) and (9) gave a satisfactory result (Fig. 2). This is probably due to the fact that the relaxation time of the first component  $\tau_1$  is too short. The resolution of the equipment used (the response time of the experimental unit) is approximately 3 times higher than  $\tau_1$ , which levels out the difference in the behavior of the Gaussian and exponential components. The relaxation characteristics of ethylene glycol also practically did not change, but the relaxation law of the first component changed.

The algorithm proposed in this work for determining the relaxation characteristics of solvents from non-stationary experimental spectra of a fluorophore is more laborious and requires significantly more time and computational resources. However, it makes it possible to noticeably improve the quality of fitting the calculated spectra to the experimental ones and significantly improve the accuracy of determining the relaxation characteristics of solvents.

Additional material can be found in the online version of ESM1.pdf

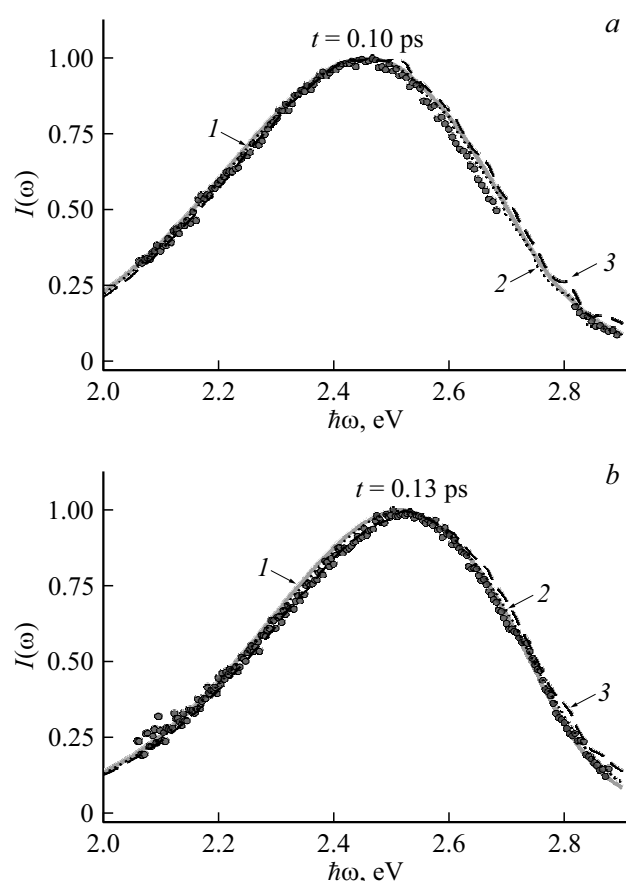


**Figure 4.** Profile of the fluorescence spectrum in DS (a), in BN (b) after a time interval of 0.10 and 0.13 ps after photo-excitation, respectively. Experimental data [24] are shown with symbols. Solid gray curve 1 is approximation using the model (9), dotted curve 2 is approximation using the model (1), dashed curve 3 is model (1) using convolution (12).

Comparison of parameters of relaxation modes of solvents

Solvent	Model	$x_1$	$x_2$	$x_3$	$\tau_1$ , ps	$\tau_2$ , ps	$\tau_3$ , ps
IP, dipropyl ether	(9) [24]	0.66	0.34		0.12	5.60	
	(1)	0.57	0.43		0.11	3.78	
EE, ethyl ether	(9) [24]	0.53	0.47		0.05	0.89	
	(1)	0.52	0.48		0.04	0.87	
EA, ethyl acetate	(9) [24]	0.41	0.32	0.27	0.08	0.53	3.1
	(1)	0.34	0.34	0.32	0.06	0.35	2.5
BN, butyronitrile	(9) [24]	0.54	0.41	0.05	0.17	1.40	18.0
	(1)	0.41	0.52	0.07	0.19	1.03	12.76
DS, dimethyl sulfoxide	(9) [24]	0.56	0.30	0.14	0.16	1.49	7.33
	(1)	0.46	0.35	0.19	0.19	0.95	6.43
	[26]	0.50	0.41	0.092	0.214	2.29	10.7
EG, ethylene glycol	(9) [24]	0.45	0.19	0.35	0.10	4.0	36.0
	(1)	0.43	0.20	0.37	0.11	3.4	35.01
	[26]	0.307	0.255	0.439	0.187	4.98	32.0

## Conclusion

Reconstruction of the relaxation characteristics of solvents from the dynamics of the fluorescence band maximum faced serious difficulties for decades due to the uncertainty of the initial position of the fluorescence band [26]. This difficulty has recently been overcome by simulating the full non-stationary fluorescence spectrum and a consistent description of the pumping process [24]. However, in the work [24] the duration of the gating pulse was completely neglected. In this work, the approach with an explicit description of the envelope of the gating pulse in the calculation of the non-stationary fluorescence spectrum, is proposed. The performed fitting of such spectra to the experimental ones showed that neglecting the finite duration of the gating pulse leads to significant errors. Based on this approach, the relaxation characteristics of a number of widely used solvents, such as ethylene glycol, dimethyl sulfoxide, butyronitrile, ethyl acetate, ethyl ether, and dipropyl ether, have been refined.

The relaxation time of intramolecular high-frequency vibrations of C153 coumarin, which are active in the  $S_0 \rightarrow S_1$  optical transition, is much shorter than the resolution of the experimental unit, and it is difficult to determine it from non-stationary experimental spectra. However, there are many molecules for which the vibrational relaxation time is much longer. This approach will make it possible to determine the relaxation time of active intramolecular vibrations of such molecules.

## Acknowledgments

The authors are grateful to Prof. G. Angulo (Institute of Physical Chemistry, Polish Academy of Sciences) and Dr. A. Rosspeintner (University of Geneva, Switzerland) for providing the experimental data, Candidate of Physical

and Mathematical Sciences (Ph.D). A.E. Nazarov for the developed software package [42].

## Funding

The study was supported by a grant from the Russian Science Foundation № 22-13-00180, <https://rscf.ru/project/22-13-00180/>.

## Conflict of interest

The authors declare that they have no conflict of interest.

## References

- [1] N.G. Bakhshiev. Opt. Spectrosc., **16**, 821 (1964). (in Russian)
- [2] Yu.T. Mazurenko, N.G. Bakhshiev. Opt. i spektr., **28** (5), 905 (1970) (in Russian).
- [3] K. Tominaga, G.C. Walker, W. Jarzeba, P.F. Barbara. J. Phys. Chem., **95** (25) 10475 (1991). DOI: 10.1021/j100178a039
- [4] A.V. Barzykin, P.A. Frantsuzov, K. Seki, M. Tachiya. Adv. Chem. Phys., **123**, 511 (2002). DOI: 10.1002/0471231509.ch9
- [5] E. Vauthey. J. Photochem. Photobiol. A, **179**, 1 (2006). DOI: 10.1016/j.jphotochem.2005.12.019
- [6] M. Glasbeek, H. Zhang. Chem. Rev., **104** (4), 1929 (2004). DOI: 10.1021/cr0206723
- [7] G. Angulo, J. Jeedrak, A. Ochab-Marcinek, P. Pasitsuparoad, C. Radzewicz, P. Wnuk, A. Rosspeintner. J. Chem. Phys., **146**, 244505 (2017). DOI: 10.1063/1.4990044
- [8] T. Kumpulainen, B. Lang, A. Rosspeintner, E. Vauthey. Chem. Rev., **117**, 10826 (2017). DOI: 10.1021/acs.chemrev.6b00491
- [9] S.V. Feskov, V.A. Mikhailova, A.I. Ivanov. J. Photochem. Photobiol. C., **29**, 48 (2016). DOI: 10.1016/j.jphotochemrev.2016.11.001
- [10] A.I. Ivanov, V.A. Mikhailova. Uspekhi khimii, **79** (12), 1139 (2010). [A.I. Ivanov, V.A. Mikhailova. Russ. Chem. Rev., **79** (12), 1047 (2010). DOI: 10.1070/RC2010v079n12ABEH004167].

- [11] T. Asahi, N. Mataga. J. Phys. Chem., **95**, 1956 (1991). DOI: 10.1021/j100158a014
- [12] E. Akesson, G. Walker, P. Barbara. J. Chem. Phys., **95** (6), 4188 (1991). DOI: 10.1063/1.460774
- [13] S.M. Swicka, W. Zhua, M. Mattaa, T.J. Aldricha, A. Harbuzaruc, J.T.L. Navarretec, R.P. Ortizc, K.L. Kohlstedta, G.C. Schatzza, A. Facchetti, F.S. Melkonyana, T.J. Marks. Proc. Nat. Acad. Sc., **115** (36) E834 (2018). DOI: 10.1073/pnas.1807535115
- [14] G.D. Tainter, M.T. Hörantner, Luis M. Pazos-Outón, R.D. Lamboll, H. Āboliņš, T. Leijtens, S. Mahesh, R.H. Friend, H.J. Snaith, H.J. Joyce, F. Deschler. Joule. **3** (5), 1301 (2019). DOI: 10.1016/j.joule.2019.03.010
- [15] A.A. Ovchinnikov, M.Ya. Ovchinnikova. ZhETF, **56** (4), 1278 (1969). [A.A. Ovchinnikov, M.Ya. Ovchinnikova. Sov. Phys. JETP, **29** (4), 688 (1969).]
- [16] H. Fröhlich. *Theory of dielectrics: Dielectric constant and dielectric loss*, 2nd ed. (Clarendon Press, Oxford, 1958).
- [17] Y. Tanimura, S. Mukamel. *Quantum brownian oscillator analysis of pump-probe spectroscopy in the condensed phase, Ultrafast Dynamics of Chemical Systems*, (Springer, Dordrecht, 1994).
- [18] S. Mukamel. Principles of Nonlinear Optical Spectroscopy, (Oxford university press, New York, 1995).
- [19] W. Domcke, G. Stock. Adv. Chem. Phys., **100**, 1 (1997). DOI:10.1002/9780470141595.ch1
- [20] D.-Y. Yang, S.-Y. Sheu. J. Chem. Phys., **106** (23), 9427 (1997). DOI:10.1063/1.473847
- [21] C.P. Koch, T. Kluner, R. Kosloff. J. Chem. Phys., **116** (18), 7983 (2002). DOI: 10.1063/1.1450124
- [22] S.A. Kovalenko, N. Eilers-Konig, T.A. Senyushkina, N.P. Ernsting. J. Phys. Chem. A, **105** (20), 4834 (2001). DOI: 10.1021/jp004007e
- [23] D. Egorova, M.F. Gelin, W. Domcke. J. Chem. Phys., **122** (13), 134504 (2005). DOI: 10.1063/1.1862618
- [24] R.G. Fedunov, I.P. Yermolenko, A.E. Nazarov, A.I. Ivanov, A. Rosspeintner, G. Angulo. J. Mol. Liq., **298**, 112016 (2020). DOI: 10.1016/j.molliq.2019.112016
- [25] A.E. Nazarov, A.I. Ivanov, A. Rosspeintner, G. Angulo. J. Mol. Liq., **360**, 119387 (2022). DOI: 10.1016/j.molliq.2022.119387
- [26] M.L. Horng, J.A. Gardecki, A. Papazyan, M. Maroncelli. J. Phys. Chem., **99**, 17311 (1995). DOI: 10.1021/j100048a004
- [27] M. Maroncelli, V.P. Kumar, A. Papazyan. J. Phys. Chem., **97**, 13 (1993). DOI: 10.1021/j100103a004
- [28] L.D. Zusman, A.B. Gelman. Opt. i spektr., **53** (3), 248 (1982) (in Russian).
- [29] A.J. Leggett, S. Chakravarty, A.T. Dorsey, M. Gary. Rev. Mod. Phys., **59** (1), 1 (1987). DOI: 10.1103/RevModPhys.59.1
- [30] A.O. Caldeira, A.J. Leggett. Ann. Phys. (N.Y.) **149** (2), 374 (1983). DOI: 10.1016/0003-4916(83)90202-6
- [31] A. Garg, J.N. Onuchic, V. Ambegaoka. J. Chem. Phys., **83** (9), 4491 (1985). DOI: 10.1063/1.449017
- [32] A.I. Ivanov, G.S. Lomakin, V.A. Mikhailova. Chem. Physics, **10** (5), 638 (1991). [A.I. Ivanov, G.S. Lomakin, V.A. Mikhailova. Soviet J. Chem. Phys., **10** (5), 972 (1992)].
- [33] A.I. Ivanov, V.V. Potovoi. Chem. Phys., **247** (2), 245 (1999). DOI: 10.1016/S0301-0104(99)00197-4
- [34] B.D. Fainberg, D. Huppert. Adv. Chem. Phys., **107**, 191 (1999).
- [35] L.D. Zusman. Chem. Phys., **49** (2), 295 (1980). DOI: 10.1016/0301-0104(80)85267-0
- [36] D.F. Calef, P.G. Wolynes. J. Phys. Chem., **87** (18), 3387 (1983). DOI: 10.1021/j100241a008
- [37] R. Kubo, Y. Toyozawa. Progress of Theoretical Physics, **13** (2), 160 (1955). DOI: 10.1143/PTP.13.160
- [38] J.-L. Chang. J. Mol. Spectrosc., **232**, 102 (2005). DOI: 10.1016/j.jms.2005.03.004
- [39] I.P. Ermolenko, V.A. Mikhailova, A.I. Ivanov. Izvestiya UNTS RAN, **27** (1), (2021) (in Russian) DOI: 10.31040/2222-8349-2021-0-1-27-32
- [40] B. Bagchi, R. Biswas. Adv. Chem. Phys., **109**, 207 (1999).
- [41] A.I. Ivanov, A.O. Kichigina. Khim. fizika, **31** (3), 3 (2012). [A.I. Ivanov, A.O. Kichigina. Russ. J. Phys. Chem. B, **6** (2), 175(2012). DOI: 10.1134/S1990793112020066]
- [42] A.E. Nazarov, A.I. Ivanov. Computer Physics Communications, **270**, 108178 (2022). DOI: 10.1016/j.cpc.2021.108178